Geometric Accuracy and Mechanical Behavior of PA6 Composite Curved Tubes Fabricated by Fused Filament Fabrication (FFF)

Mohammadali Shirinbayan, Khaled Benfriha, Abbas Tcharkhtchi

Geometric Accuracy and Mechanical Behavior of PA6 Composite Curved Tubes Fabricated by Fused Filament Fabrication (FFF)

Mohammadali Shirinbayan, Khaled Benfriha, and Abbas Tcharkhtchi*

Herein, the effect of processing parameters including infill pattern and reinforcement type on the dimensional accuracy of products manufactured by the fused filament fabrication (FFF) process as well as the mechanical performance is studied. The reinforcements used to manufacture the PA6 composite are carbon, Kevlar, and glass fibers. The compression properties of the stated composites are compared. The results show that the rectangular fill pattern is less deformed compared with triangular, hexagonal, and solid ones. However, the compression strength is decreased by changing the infill pattern from the solid infill to hexagonal, triangular, and rectangular. Although there is no significant difference in terms of compression behavior, the printed PA6 reinforced with carbon fiber which is deformed outward contrary to Kevlar and glass fibers, which are deformed inward. Finally, the results confirm that the selection of the appropriate types of reinforcements and infill patterns among the several available types during the printing process is effective in improving the mechanical properties and also in providing better geometrical quality of the surfaces and the consequent dimensional precision improvement of the parts printed by the FFF process.

1. Introduction

Additive manufacturing (AM), 3D printing and prototyping, or solid freeform fabrication are all instances of a layer-by-layer manufacturing process in which parts are manufactured from designed geometries. Given the modern technological progress, AM has been gaining popularity, which can make it a common manufacturing process.[1,2] This approach has provided many benefits; it can improve flexibility and convenience, reduce manufacturing costs, and reduce turnout time for multiple manufacturing applications.[3,4] However, surface quality, accuracy, and precision have been among the main obstacles, which prevented the presence and use of AM as a primary production process.[5,6]

Among the different processes of AM, fused filament fabrication (FFF) technology is based on manufacturing parts that can be fabricated from computer-aided design (CAD) data by fusing a superposition of thin coils of filament through a heated nozzle, via layer by layer.[7] Some thermoplastic polymers used in this method are polypropylene (PP), acrylonitrile butadiene styrene (ABS), polyethylene (PE), polylactic acid (PLA), polycarbonate (PC), polyamide (PA or Nylon), polyetherimide (PEI), polyetheretherketone (PEEK), etc.[8,9]

Most of the industries are looking for stronger and lighter materials. Therefore, polymer matrix composites (PMCs) have been studied by many researchers,[10] as they can achieve the suitable thermomechanical properties when the appropriate reinforcement is used to reinforce the polymer matrix.[11] For more than a decade, the study and research on the improvement and development of composite materials for AM processes has been ongoing.[12] However, as some polymers cannot reach the required mechanical properties through AM, the FFF manufacturing process of PMCs is developed to obtain composite-based structural components with satisfactory mechanical properties for specific applications.[13–15] This method was successfully implemented by MarkForged. In fact, continuous fiber reinforcement has been introduced into 3D geometry via the double-extrusion method.[16,17]

Selecting the suitable infill pattern is an important step in producing 3D geometries. The effects of the infill percentage and infill patterns on the tensile strength of the printed ABS parts were investigated by Škrlová et al.,[18] Baich et al.,[19] and Akhoundi et al.[20] Christiyan et al.[21] investigated the effects of layer height and print speed on the FFF process reinforced ABS by hydrous magnesium silicate composite. The different layer height values of 0.2, 0.25, and 0.3 mm and also the different printing speed values of 30, 40, and 50 mm s^{-1} were considered to evaluate the impact of the stated processing parameters on the mechanical behavior of the final printed samples. The maximum mechanical behaviors were obtained by selecting 0.2 mm as layer thickness and also 30 mm s^{-1} as printing speed.

M. Shirinbayan, A. Tcharkhtchi
Arts et Metiers Institute of Technology
CNAM
PIMM
HESAM University
F-75013 Paris, France
E-mail: mohammadali.shirinbayan@ensam.eu
K. Benfriha
Arts et Metiers Institute of Technology
LCPI
HESAM University

The mechanical properties of the manufactured parts can be significantly improved by the suitable adjustment of the process parameters obtained from the conducted research.[22] It is understood that there is a clear relationship between the selected and excerpted parameters and the obtained mechanical properties of the manufactured part. Optimization of process parameters has significantly attracted the attention of different researchers, such as filling velocity (Ning et al., 2017),[23] diameter of the nozzle used, envelope temperature (Sun et al., 2008),[24] raster angle (Chockalingam et al., 2016),[25] layer thickness (Lee et al., 2005),[26] road width (Anitha et al., 2001, Duigou et al., 2016),[27,28] raster gap (Mohamed et al., 2016), and[29] temperature of extrusion (Garg and Singh, 2016, Boparai et al., 2016).[30,31] All these parameters should be controlled to achieve a suitable part quality with satisfactory mechanical properties.

Besides the stated mechanical issue of the FFF process, the control of the required dimensional accuracy is another controversial issue for the application of the FFF process in direct manufacturing.[32–34] Multiple variation sources can cause shape deviation and inaccuracy of AM components in comparison with the desired and designed shapes. Several research studies on optimization of the required geometric accuracy of the manufactured parts via FFF processes have been conducted. According to the Bochmann et al.'s[35] investigation, it is stated that the magnitude of the errors significantly varied in the x, y, and z directions in the FFF process, which can influence the accuracy, precision, and quality of the final surface. El-Katatny et al.[36] measured and analyzed the error obtained in the geometric characteristics of the determined sections on anatomical parts which have been manufactured by the FFF process. A methodology of the spectral graph theory was used by Tootooni et al.[37] and Rao et al.[38] to quantify and evaluate the geometric precision of FFF parts using the deviations of the 3D point cloud coordinate measurements from the specifications of the design. It was clarified that the proposed indicator did not propose a relationship or correlation between the geometric precision and the process parameters but only facilitated the comparison of the geometric precision of the parts. Statistical analysis of dimensional accuracy is based on the Taguchi method and artificial neural network (ANN). Sood et al.[39] optimized the processing parameters including layer thickness, part orientation, and raster angle in FFF. Saqib et al.[40] reported that the geometry of an object affects the accuracy more than the processing parameters in the FFF process. Also, the perpendicularity and flatness features of geometries could influence the accuracy of the printed components. Chang et al.[41] found that profile errors and extruding apertures are two essential quality factors which need to be taken into account via the FFF process. Also, the accuracy depends on transmission machinery and filament diameter.

The choice of the appropriate type of the reinforcements and infill patterns during the printing process is effective in improving the mechanical properties and in providing a dimensional precision improvement of the parts printed by the FFF process. This study assesses and characterizes the influence of the process parameters including material type and the selected infill pattern on the dimensional accuracy, as well as on the mechanical properties of the parts manufactured by the FFF process. After the Experimental Section, the different parameters of the FFF process are to produce PA6 composite curved tubes. After that, the geometric accuracy measurement results of PA6 composites curved tubes are presented. A compression test was applied on the printed PA6 with different infill patterns and PA6 reinforced with carbon, Kevlar, and glass fibers under uniform conditions, and the mechanical performances of all three composite types are compared.

2. Experimental Section

2.1. Raw Materials

The material used as raw material was polyamide 6 (PA6). It was introduced as one of the newest matrix materials for fabricating the composite parts with Markforged 3D printers. The isotropic fiber fill type made of carbon, glass, and Kevlar was chosen as the reinforcement printing type. The filament diameter was 1.75 mm. The printed model for this study was a tube with height, thickness, and external diameter of 50, 4, and 40 mm, respectively (**Figure 1**). PA6 used had a density of 1.14 g cm^{-3} and melt mass flow rate of 3 g/10 min. Some characteristics of carbon, Kevlar, and glass fibers (the reinforcements) are presented in **Table 1**.

2.2. 3D Printer Device

One of the Markforged desktop printers is Mark Two Printer, which was used in this study. This printer was used to print parts from PA6 supplied by Markforged. It allowed reinforcing parts with continuous carbon, glass, or Kevlar fibers.

PA6 was printed with a temperature of 273 °C and fiber layers were printed with a temperature of 232 °C, on a nonheated printer bed platform. The carbon fiber was printed in a layer height value of 0.125 mm, and the Kevlar and glass fibers used were printed with a layer height of 0.1 mm. The dual extrusion system allowed continuous fiber reinforcements to be placed as

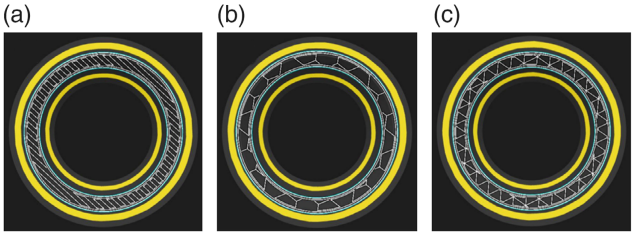

Figure 1. Schematic of different filling patterns: a) rectangular, b) hexagonal, and c) triangular.

Table 1. Some characteristics of carbon, Kevlar, and glass fibers.

Continuous fiber	Carbon	Kevlar	Glass
Density [g cm^{-3}]	1.4	1.2	1.5
Heat deflection temperature [°C]	105	105	105
Compressive strength [MPa]	320	97	140
Compressive modulus [MPa]	54	28	21

the required and determined layers. Also, this possibility was provided to specify the fiber orientation in the component during the deposition process. Eiger was the designated software for MarkTwo, which made it possible to import OBJ and STL models.

Mark Two can produce different structures at different percentages. According to the related printer software, it was possible to choose three main types of infill patterns, which were rectangular, triangular, and hexagonal. Also, during our study, we considered the solid infill status as another structure or infill pattern. In fact, in the solid fill pattern, the raster orientations of the layers were $+45^{\circ}$ and -45°. Concentric and isotropic were the fiber patterns that could be selected in the Markforged Mark Two desktop 3D printer.

Moreover, two types of specimens were considered: unreinforced and continuous reinforced PA6 specimens. The printing conditions for the polymer (PA6) samples were 37% of fill density for the triangular and rectangular, hexagonal fill patterns, four roof and layers (the number of layers of solid plastic were used on the top and bottom of the part), and two wall layers (the thick walls of the part). More walls will make a pure plastic part stronger, but will also reduce the area that the fiber will be able to fit into. For the solid fill pattern, the density was 100% with two wall layers. For PA6, full reinforced (carbon, glass, and Kevlar) specimens were printed with the solid fill pattern,100% fill density, four roof and layers, and two wall layers. The total fiber layer was 490 (the total number of layers filled with fibers) with a concentric fiber fill type (the fiber fill type determined the algorithms which controlled how fiber was used to reinforce the part). All the walls were reinforced (inner holes and outer shell) and two concentric fiber rings were added (the number of rings of concentric fiber fill added per layer). **Table 2** indicates the processing parameters information.

2.3. Characterization Methods

2.3.1. Geometric Accuracy Measurement

A desktop 3D laser scanner (Solutionix D500) that excels at scanning small, intricate objects and the most complicated goods was used. The scan speed of this equipment was high speed due to the strong engines. It had a resolution of 0.055 mm and a precision of 0.01 mm. The geometry and obtained point-by-point coordinate measurements of the component, referred to as a 3D point cloud, were prepared by the scanner. The laser scanner recorded reflected light from the part surface as a point in the 3D space, with a maximum volumetric deviation. Solutionix D500 was powered by Solutionix ezScan. The program was used to calibrate devices as well as process scan data stitch images taken from different sides at different angles. The desktop rotated scanned objects from different angles. A ray of blue light bounced off objects and entered camera lenses.

For dimensional and quality control, a professional 3D Geomagic Control X software was used, which captured and processed data from 3D scanners. It made possible calculation of geometric deviations by comparing the data from the point cloud with the original CAD model. The calculation procedure consisted of several steps. The alignment of the measured scan to the CAD required a careful part alignment procedure to achieve consistent results. The alignment step required matching at least four points of the raw point cloud data to the CAD model and subsequent analysis, each of which has its own literature.[24,25]

2.3.2. Quasistatic Compression Test

The sample used was according to Figure 1. Quasistatic compression experiments were achieved with the INSTRON 5966 machine, a loading cell of 50 kN, and the loading speed used was 5 mm min^{-1}. The special jaws were designed to perform the compression tests and the tubes were positioned between two jaws. To ensure reproducibility of the results, at least three samples were created in the compression test study.

3. Results and Discussion

The tubes were printed using the PA6 filament and continuous fibers, under the main stated fill patterns. Then they were

Table 2. 3D printing conditions.

Material		Polymer infill (PA6)		Composite infill PA6 (GF, CF and K)	
Infill	Fill pattern	Triangular rectangular hexagonal	Solid	Triangular rectangular hexagonal	Solid
	Fill density	37%	100%	100%	
	Roof and floor layers	4	–	4	4
	Reinforcement	–		Upper and lower surface only	Full reinforcement
	Wall layers	2		2	2
	Total fiber layers			8	490
	Fiber fill type	–		Isotropic	Concentric
	Walls to reinforce			–	All walls
	Fiber angles			0, 45, and 90°	–
	Concentric fiber rings			2	2

analyzed for geometric accuracy. Finally, the tubes were tested under compression loading. The comparison with the compression strength of the different patterns and also with the solid pattern, for which fill percentage was 100%, was carried out. So, the compression strength was considered as the criterion to make the comparison.

3.1. Effect of Infill Patterns

This part treats three important parameters; the first parameter is the choice of materials: PA6, which has been used as a matrix, and also composites, PA6 reinforced with three types of fibers which are carbon fiber, glass fiber, and Kevlar. The second parameter is infill pattern: triangular, and rectangular, hexagonal, solid. These parameters were varied to investigate which parameter affects the dimensional accuracy the most and what are the more appropriate for a better print quality and high precision accuracy. One of the printed sample is shown in **Figure 2**.

Geometric accuracy results for PA6 with different fill patterns, triangular, rectangular, hexagonal, and solid, are presented in **Figure 3**. One can see that the parts (specimens) are deformed inward, which is known as the shrinkage phenomenon and with different amplitudes (**Figure 4**). The rectangular fill pattern is less deformed compared with triangular, hexagonal, and solid ones. It can be noted that by the printing orientation of $+45°/-45°$, the symmetric geometry is more possible for rectangular fill pattern. The later can be related to the homogeneous cooling rate in the rectangular fill pattern. One can note that from 10 to 40 mm of the height of tube for all fill patterns, there is homogenous deformation. At the initial time of printing (from 0 to

Figure 2. A figure of the fabricated cylindrical part.

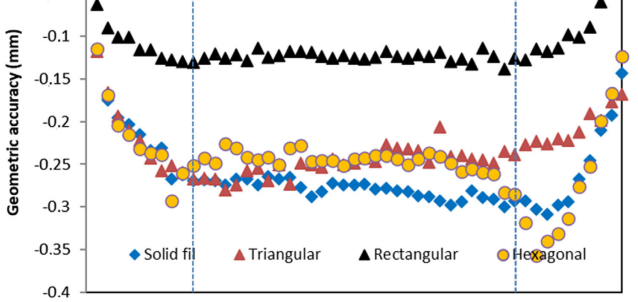

Figure 3. Geometric accuracy results for PA6 with different fill patterns.

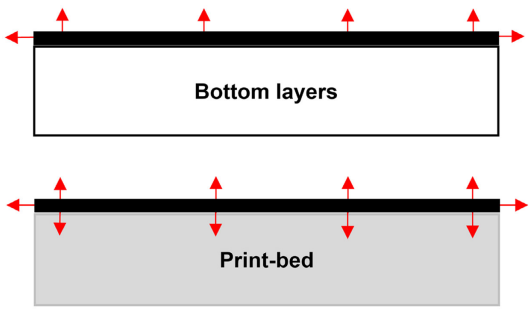

Figure 4. Shrinkage during printing of the first and last layers.

10 mm of height), the first layers can exchange temperature in all directions and the ending time of printing (from 40 to 50 mm of height) last layers, which can also exchange with air but also receives heat exchange from previous layers. Also, due to the greater number of nodes in the rectangular pattern than the triangular and hexagonal filling patterns, the deformation is less because the more nodes, the more adhesion the piece will have.

Moreover, an increasing gap with retraction of each layer and also the retraction of the lower layer which will add up is significant (**Figure 5**).

The compression test results for the different infill pattern samples, which were made of PA6, are presented in **Figure 6**. According to the comparison between the effect of the different infill patterns in the case of compression strength, the solid infill pattern had the highest strength, which was about 52.37 ± 3.5 MPa. Then, the compression strength was decreased by changing the infill pattern from the solid infill to hexagonal, triangular, and rectangular.

The related compression strengths of the printed specimens with the infill patterns of hexagonal, triangular, and rectangular were 51.02 ± 5, 28.73 ± 0.5, and 23.42 ± 2.3 MPa, respectively (**Figure 7**). In fact, by changing the infill pattern from solid infill to hexagonal infill, the compression strength was decreased by about 2.58%. However, in the case of the infill pattern change from solid to triangular and solid to rectangular, the compression strength was decreased by about 45.14% and 55.28% respectively. One can note that the number of nodes in the rectangular infill pattern is lower than the other infill patterns. This parameter is important for the structure under compression loading.

One can notice that the rectangular infill pattern has minimum compression properties; however, after geometric accuracy results, it presents minimum deformation. The latter can be explained by the relation time of the polymer used. Cooling speed of the filament for different infills can be another reason.

The temperature selection is highly influenced by the viscosity of the polymer and should be adjusted with the right printing speed; too high temperature may cause a reduction in the polymer viscosity and the melt will become very fluid and highly flowable, which results in a lot of plastic leaking out from the hot end (nozzle) during printing and reducing the dimensional accuracy. Otherwise when the temperature is too low, the new layer will

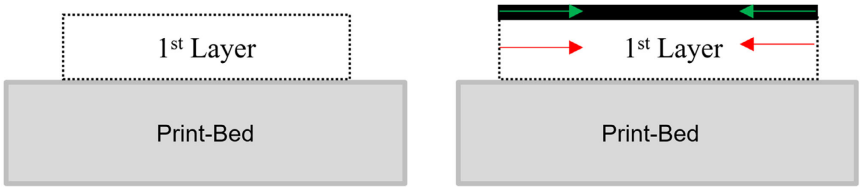

Figure 5. Cumulative shrinkage.

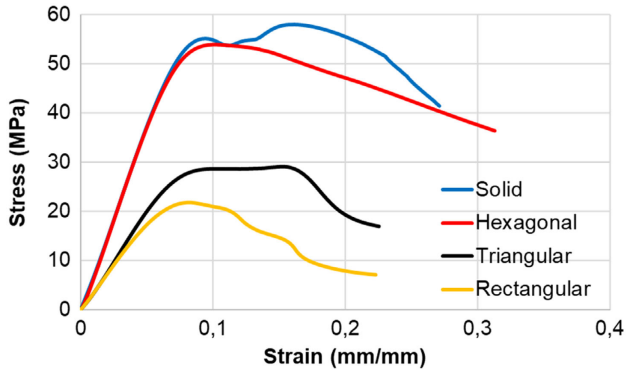

Figure 6. Compression curves for PA6 with different infill patterns.

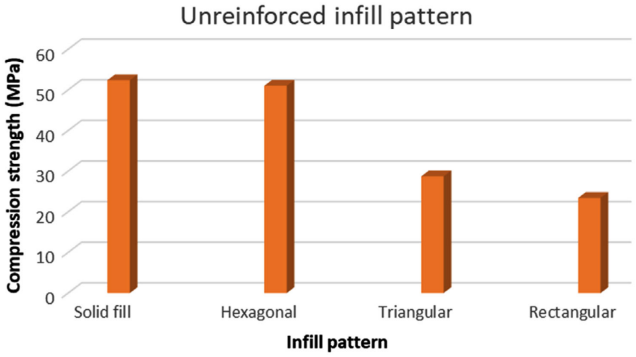

Figure 7. Compression strength of the different infill patterns.

simply not stick to the previous layer and the surface of the thread could be a bit rough.

Figure 8 presents the macroscopic view of the specimens after the compression test. The rectangular sample was found to be damaged more significantly in macroscopic observations.

3.2. Effect of Reinforcement Type

The geometric accuracy results for composite specimens (**Figure 9**) show different deformations. The printed PA6 reinforced with carbon fiber composite is deformed outward (dilatation) contrary to Kevlar and glass fiber which are deformed inward (shrinkage). Also, Kevlar is more deformed in the first layers. As the graph shows, the deformation of the reinforced tube with Kevlar and glass fiber is almost the same. The results showed different part behaviors after the FFF process, and the deformation of the measured parts (3D models) changed with the variation of reinforcement. It is important to take into account the reinforcement filament thickness: carbon fiber was printed with a layer height value of 0.125 mm, and the Kevlar and glass fibers were printed with a layer height of 0.1 mm, so it is logical to obtain this significant difference in deformation.

According to the comparison between the compression strength of the reinforced Solid infill pattern (perpendicular to the applied stress direction) by different types of the used reinforcements, glass reinforcement had the highest strength which was about 52.7 ± 2.84 MPa (**Figure 10**).

Then, the compression strength was decreased by altering the glass fibers with Kevlar and carbon fibers. The related compression strengths of the reinforced solid infill pattern by the glass, Kevlar, and carbon reinforcements perpendicular to the applied stress direction were 52.7 ± 2.84, 51.99 ± 2.95, and 49.1 ± 1.04 MPa, respectively (according to **Figure 11**). In fact, the compression strength of the reinforced PA6 (solid infill pattern) by carbon fibers was decreased by altering with Kevlar and carbon fibers at about 1.3% and 6.8%, respectively.

Although there is no significant difference between these results, one can note that the PA6 reinforced with carbon fiber has minimum compression properties in comparison with Kevlar and glass fibers. The cooling rate of the specimens through

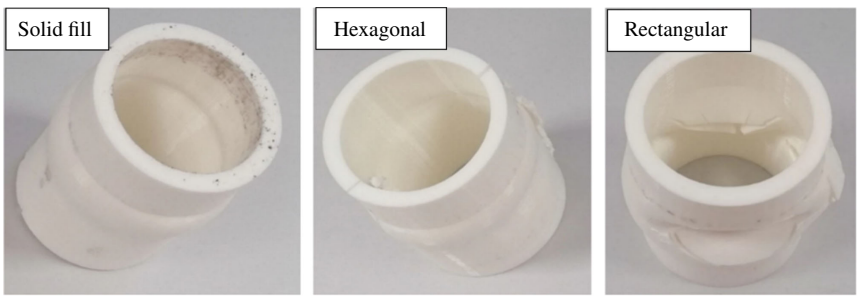

Figure 8. Macroscopic observation of tubes after compression tests.

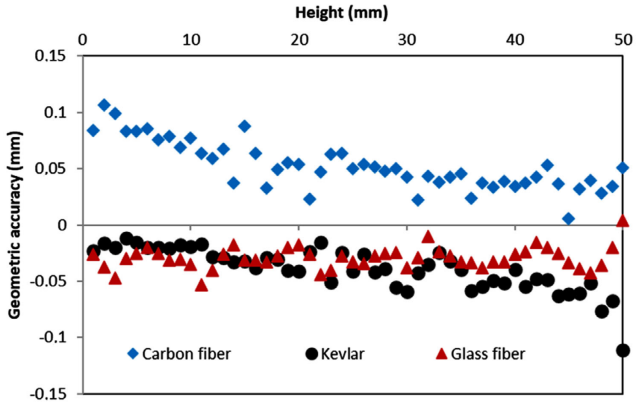

Figure 9. Geometric accuracy results for PA6 with different reinforcements.

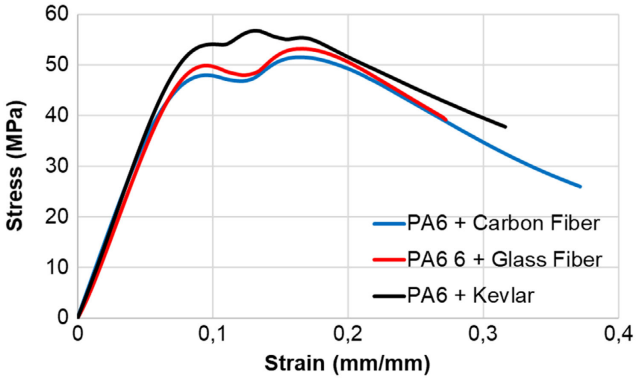

Figure 10. Compression curves for PA6 with different reinforcements.

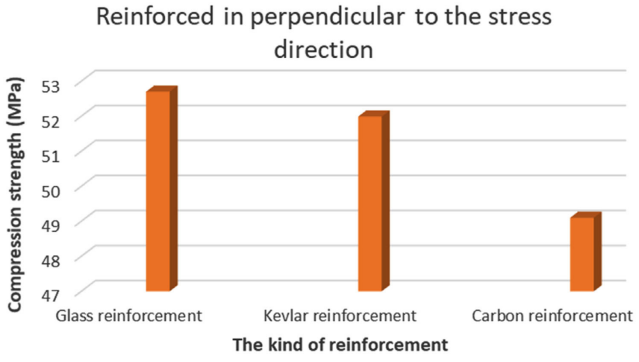

Figure 11. The effect of the different reinforcements on the compression strength (reinforcing, perpendicular to the stress direction).

the printing process is affected by the movement of the extrusion head temperature (which is higher than the envelope temperature); as a consequence, it will influence the adhesion and bonding between the adjacent deposited filament. The use of various materials in a dedicated and optimized system may change its standard melt rheological behavior requirement, thereby influencing the melt processes. Therefore, many parameters need to be adjusted to obtain the best quality for the final product.

4. Conclusion

In this study, the assessment of the influence of the process parameters including material and infill pattern on the dimensional accuracy and precision, as well as on the mechanical properties of components manufactured by the FFF process, was examined. This involves the manufacturing of PMCs with carbon, Kevlar, and glass fiber reinforcements, provided by MarkForged. Then, the compression performance of the manufactured composites was evaluated and compared. The results demonstrated that the rectangular fill pattern is less deformed compared with triangular, hexagonal, and solid ones. However, the solid infill pattern showed more compression strength. Compression strength was decreased by changing the infill pattern from hexagonal to triangular and rectangular, respectively. The results confirmed that there is no significant difference in terms of compression behavior for the printed PA6 reinforced with carbon fiber, Kevlar, and glass fiber. However, the printed PA6 reinforced with carbon fiber is deformed outward contrary to Kevlar and glass fibers which are deformed inward. One can conclude that the reinforcements and the infill patterns make it possible to improve the mechanical behavior while also obtaining better geometrical quality and precision of the FFF-manufactured parts.

Conflict of Interest

The authors declare no conflict of interest.

Author Contributions

K.B., M.S., and A.T. constructed the idea. K.B., M.S., and A.T. analyzed the results, draft manuscript preparation, and wrote the paper. M.S. corrected the English and the paper format.

Data Availability Statement

The data that support the findings of this study are available in the supplementary material of this article.

Keywords

composites, fused filament fabrication, geometric accuracies, mechanical performances, PA6

Received: August 21, 2021
Revised: January 25, 2022
Published online: May 17, 2022

[1] Y. Huang, M. C. Leu, J. Mazumder, A. Donmez, *J. Manuf. Sci. Eng.* **2015**, *137*, 525.
[2] N. Zirak, M. Shirinbayan, M. Deligant, A. Tcharkhtchi, *Polymers* **2022**, *14*, 97.
[3] B. Shaqour, M. Abuabiah, S. Abdel-Fattah, A. Juaidi, R. Abdallah, W. Abuzaina, M. Qarout, B. Verleije, P. Cos, *Int. J. Adv. Manuf. Technol.* **2021**, *114*, 1.
[4] D. L. Bourell, J. J. Beaman, M. C. Leu, D. W. Rosen, *Proc. RapidTech.* **2009**, pp. 24–5.

[5] J. I. Aguilar-Duque, J. L. García-Alcaraz, J. L. Hernández-Arellano, *Int. J. Adv. Manuf. Technol.* **2020**, *109*, 171.
[6] S. Terekhina, T. Tarasova, S. Egorov, L. Guillaumat, M. L. Hattali, *Int. J. Adv. Manuf. Technol.* **2020**, *111*, 93.
[7] J. Marchewka, J. Laska, *Int. J. Adv. Manuf. Technol.* **2020**, *106*, 4933.
[8] B. Leutenecker-Twelsiek, J. Ferchow, C. Klahn, M. Meboldt, *Int. Conf. Addit. Manuf. Prod. Appl.*, **2017**. p. 337–46.
[9] N. Zirak, M. Shirinbayan, S. Farzaneh, A. Tcharkhtchi, *Polym. Adv. Technol.* **2021**.
[10] C. Pandelidi, S. Bateman, S. Piegert, R. Hoehner, I. Kelbassa, M. Brandt, *Int. J. Adv. Manuf. Technol.* **2021**, *113*, 1.
[11] C. González, J. J. Vilatela, J. M. AldareguíaMolina-, C. S. Lopes, J. LLorca, *Prog. Mater. Sci.* **2017**, *89*, 194.
[12] A. P. Sobha, P. S. Sreekala, S. K. Narayanankutty, *Prog. Org. Coatings* **2017**, *113*, 168.
[13] N. Mohan, P. Senthil, S. Vinodh, N. Jayanth, *Virtual Phys. Prototyping* **2017**, *12*, 47.
[14] N. Abbasnezhad, N. Zirak, M. Shirinbayan, A. Tcharkhtchi, F. Bakir, *J. Drug Delivery Sci. Technol.* **2021**, *63*, 102446.
[15] N. G. Karsli, A. Aytac, *Composites Part B Eng.* **2013**, *51*, 270.
[16] E. C. Botelho, M. C. Rezende, B. Lauke, *Composites Sci. Technol.* **2003**, *63*, 1843.
[17] G. W. Melenka, B. K. O. Cheung, J. S. Schofield, M. R. Dawson, J. P. Carey, *Compos. Struct.* **2016**, *153*, 866.
[18] K. Škrlová, K. Malachová, A. Muñoz-Bonilla, D. Měřinská, Z. Rybková, M. Fernández-García, D. Plachá, *Nanomaterials* **2019**, *9*, 1548.
[19] L. Baich, G. Manogharan, H. Marie, *Int. J. Rapid Manuf.* **2015**, *5*, 308.
[20] B. Akhoundi, A. H. Behravesh, *Exp. Mech.* **2019**, *59*, 883.
[21] K. G. J. Christiyan, U. Chandrasekhar, K. Venkateswarlu, *IOP Conf. Ser. Mater. Sci. Eng.* **2016**, *114*, 12109.
[22] H. R. Vanaei, K. Raissi, M. Deligant, M. Shirinbayan, J. Fitoussi, S. Khelladi, A. Tcharkhtchi, *J. Mater. Sci.* **2020**, *55*, 14677.
[23] F. Ning, W. Cong, Y. Hu, H. Wang, *J. Compos. Mater.* **2017**, *51*, 451.
[24] Q. Sun, G. M. Rizvi, C. T. Bellehumeur, P. Gu, *Rapid Prototyping J.* **2008**, *14*, 72.
[25] K. Chockalingam, N. Jawahar, J. Praveen, *Mater. Manuf. Process.* **2016**, *31*, 2001.
[26] B. H. Lee, J. Abdullah, Z. A. Khan, *J. Mater. Process. Technol.* **2005**, *169*, 54.
[27] R. Anitha, S. Arunachalam, P. Radhakrishnan, *J. Mater. Process. Technol.* **2001**, *118*, 385.
[28] A. Le Duigou, M. Castro, R. Bevan, N. Martin, *Mater. Des.* **2016**, *96*, 106.
[29] O. A. Mohamed, S. H. Masood, J. L. Bhowmik, *Mater. Manuf. Process.* **2016**, *31*, 1983.
[30] H. Garg, R. Singh, *Rapid Prototyping J.* **2016**, *22*, 338.
[31] K. S. Boparai, R. Singh, H. Singh, *Rapid Prototyping J.* **2016**.
[32] G. Navangul, R. Paul, S. Anand, *J. Manuf. Sci. Eng.* **2013**, *135*, 18.
[33] Q. Huang, H. Nouri, K. Xu, Y. Chen, S. Sosina, T. Dasgupta, *2014 IEEE Int. Conf. Autom. Sci. Eng.* IEEE, Piscataway, NJ **2014**. p. 25–30.
[34] Z. Shakeri, K. Benfriha, M. Shirinbayan, M. Ahmadifar, A. Tcharkhtchi, *Polymers* **2021**, *13*, 3697.
[35] L. Bochmann, C. Bayley, M. Helu, R. Transchel, K. Wegener, D. Dornfeld, *Surf. Topogr. Metrol. Prop.* **2015**, *3*, 14002.
[36] I. KatatnyEl-, S. H. Masood, Y. S. Morsi, *Rapid Prototyping J.* **2010**, *16*, 36.
[37] M. S. Tootooni, A. Dsouza, R. Donovan, P. K. Rao, Z. Kong, P. Borgesen, *Int. Manuf. Sci. Eng. Conf.*, American Society of Mechanical Engineers, **2017**, p. V002T01A042.
[38] P. K. Rao, Z. Kong, C. E. Duty, R. J. Smith, V. Kunc, L. J. Love, *J. Manuf. Sci. Eng.* **2016**, *138*, 064701.
[39] A. K. Sood, R. K. Ohdar, S. S. Mahapatra, *Mater Des.* **2009**, *30*, 4243.
[40] S. Saqib, J. Urbanic, *Enabling Manufacturing Competitiveness and Economic Sustainability*, **2012**. p. 293.
[41] D.-Y. Chang, B.-H. Huang, *Int. J. Adv. Manuf. Technol.* **2011**, *53*, 1027.